NASA Technical Memorandum 83428

Vibration in Planetary Gear Systems With Unequal Planet Stiffnesses

J. L. Frater and R. August
Cleveland State University
Cleveland, Ohio

and

F. B. Oswald
Lewis Research Center
Cleveland, Ohio

Prepared for the
Eighth Applied Mechanisms Conference
sponsored by Oklahoma State University
St. Louis, Missouri, September 19-21, 1983

NASA

VIBRRATION IN PLANETARY GEAR SYSTEMS WITH UNEQUAL PLANET STIFFNESSES

J. L. Frater and R. August*
Cleveland State University
Cleveland, Ohio

and

F. B. Oswald
National Aeronautics and Space Administration
Lewis Research Center
Cleveland, Ohio

E-1716

Summary

An algorithm suitable for a mini-computer was developed for finding the natural frequencies and mode shapes of a planetary gear system which has unequal stiffnesses between the sun/planet and planet/ring gear meshes. Mode shapes are represented in the form of graphical computer output that illustrates the lateral and rotational motion of the three co-axial gears and the planet gears. This procedure permits the analysis of gear trains utilizing non-uniform mesh conditions and user specified masses, stiffnesses, and boundary conditions. Numerical integration of the equations of motion for a three planet system was performed. Excellent agreement was obtained between natural frequencies calculated assuming constant mesh stiffnesses and resonant frequencies of the dynamic system. The algorithm can be used for determining the time step and total integration times in the numerical solution of the differential equations of motion. The methodology is a quick and efficient means of identifying operating resonance regions and analytically tuning the drive train by examining the effect of parameters such as planet and sun gear support stiffnesses, input/output shaft stiffnesses, and gear mesh stiffnesses. The algorithm is adaptable for use in a Computer-Aided Design (CAD) environment.

Nomenclature

F_x	force in x-direction, N (lb)
F_y	force in y-direction, N (lb)
j	planet index
K	translational support stiffness, N/m (lb/in)
KPR	planet/ring mesh stiffness, N/m (lb/in)
KSP	sun/planet mesh stiffnesses, N/m (lb/in)
KT	torsional support stiffness, N/m (lb/in)
R	base circle radius, m (in)
T	torque, N m (lb in)
α	angle of line of action for sun/planet mesh (see Fig. 4)
β	planet reference angle (see Fig. 4)
γ	angle of line of action for planet/ring mesh (see Fig. 6)
ϕ	gear pressure angle (see Fig. 4)

Introduction

Many advanced technology applications in power transmissions, such as aircraft applications, have a high power to weight ratio requirement. Planetary gear trains, rather than parallel shaft transmissions, are widely used for these applications because of a considerable savings in weight, space and drive train efficiency. These advantages stem from the fact that multiple planets allow the load to be transmitted by several tooth contacts. For a planetary arrangement with three planets, each tooth engagement of the sun gear must carry only one third of the total static load. Consequently, the dimension of the sun gear may be considerably reduced from that of the pinion of a parallel shaft gear designed to transmit an equivalent torque. Furthermore, the co-axial arrangement of driven and driving shafts allows a compact layout.

The analytical determination of the natural frequencies of planetary gear trains is an important design criteria for three reasons. First, in addition to considering the input/output speeds of the transmission, the power transmitted and tooth loads and stresses, the designer must take care to assure that he does not excite a natural frequency within the power transmission system. This may lead to a fatigue problem and eventual premature failure of a drive train component.

Secondly this algorithm provides the designer with a tool with which he can analytically "tune" his drive train. He may interactively modify important drive train parameters such as the stiffnesses of the planet-ring mesh, planet support, input/output shaft and transmission housing.

A third reason, and the one that initiated the research documented here, is to provide a basis for selecting a time step for the numerical integration of the equations of motion of the planetary gear train. This integration is important in determining the dynamic loads, and stresses. Judicious selection of the time step assures the stability of the integration process.

Several investigators have considered the natural frequencies of planetary gear trains having equally loaded/equal stiffness planet meshes. Cunliffe, et al.[1] was successful in correlating results from an experimental test rig and analog computer analyses to analytical determinations. Using these approaches, they modeled simple planetary gear trains as well as some complex designs considering linear and nonlinear mesh stiffness. Their investigation was limited to a star gear system with a stationary carrier and a rotating annulus. This resulted in a system having 13 kinematic degrees of freedom.

Botman[2] extended this work to an eighteen degree of freedom model that included the effects

*R. August is presently employed by Life Systems, Inc., Cleveland, Ohio.

of planet pin stiffness and rotation of the carrier. It is the objectives of the analysis reported herein to (a) extend Botman's work to include unequal mesh stiffness between the three planets in the sun-planet and/or planet-ring meshes, (b) to analyze the effect of a thin tooth in one of the components and (c) to simulate unequal stiffnesses due to alternation between one and two pairs of teeth in contact.

Dynamic Model

Background

This analysis is limited to the free in-plane vibration (undamped) of a single-stage, multiple-planet system such as the one illustrated in Fig. 1. While all of the figures illustrate a three-planet system, the method is directly applicable to systems with any number of planets. Components are treated as lumped-parameter rigid bodies. The generalized Jacobi eigenvalue routine used requires symmetrical inertia and stiffness matrices, therefore, a global coordinate system is required. The general model shown in Figs. 2 and 3 involves 18 degrees of freedom: three for each component (one rotational, two translational). The components include sun gear, ring gear (annulus), carrier, and three planets. Simpler models involving fewer degrees of freedom can be simulated by suppressing unwanted modes with extremely high values of the support stiffness parameter.

Each member is modeled as supported by a torsional spring of stiffness KT and a bearing support of two equal springs of stiffness K located along the X-Y coordinates axes. (Note: For the planets, KT is zero.) Gear mesh interactions (which are treated as parameters) are modeled as linear springs of constant stiffness acting tangentially at the respective base circles. The support springs and mesh interactions are shown in Fig. 3 (only one planet is shown). Constant tooth stiffnesses permit a linear stiffness matrix and a manageable eigenroutine. Botman[2] states that this approach predicts realistic frequencies and mode shapes. Calculation of dynamic tooth loads (not considered in this model) requires time varying stiffnesses to account for the alternation between one and two pairs of teeth in contact at each mesh interaction.

Equations of Motion

The equation of motion for an n-degree of freedom system in free vibration is:

$$[M]\{\ddot{q}\} + [C]\{\dot{q}\} + [K]\{q\} = \{0\} \qquad (1)$$

where M is the inertia (mass) matrix, C is the damping matrix (assumed zero), K is the stiffness matrix and q is the vector of the generalized coordinates (θ, x, y) for each component. For the lumped mass system here, the inertia terms form a diagonal (uncoupled) matrix and the stiffness matrix is symmetric. The stiffness terms shown in Table 1 are developed by calculating the reaction (torque or force) resulting from a unit relative displacement, q, in each coordinate direction (θ, x, y) for each component. Component interactions are shown in Figs. 4 to 6.

Assembly of Inertia and Stiffness Matrices

The diagonal inertia matrix is composed of the mass moment of inertia term and two equal mass terms (representing the three degrees of freedom) for each component. The negative of each reaction term is assembled into a stiffness matrix by taking the terms in systematic order consistant with the order used in the inertia matrix. While any consistant ordering of terms may be used, a logical ordering with directly interacting components placed adjacent to each other minimizes the band width of the eigenproblem. This produces faster convergence and improved accuracy. The components are ordered: Sun, planet 1, planet 2, ..., planet n, carrier, and ring. The three degrees of freedom for each component are taken in order: θ, x, y. Thus, the stiffness matrix includes:

$$\begin{bmatrix} K_{S_\theta S_\theta} & K_{S_\theta S_x} & K_{S_\theta S_y} & K_{S_\theta 1_\theta} & K_{S_\theta 1_x} & \cdots & K_{S_\theta R_y} \\ K_{S_x S_\theta} & K_{S_x S_x} & \cdots & & & & \\ K_{S_y S_\theta} & K_{S_y S_y} & K_{S_y S_y} & \cdots & & & \\ \cdots & & & K_{1_\theta 1_\theta} & & & \\ K_{R_y S_\theta} & \cdots & & & & & K_{R_y R_y} \end{bmatrix} \qquad (2)$$

Each diagonal term of the stiffness matrix also includes the appropriate bearing support reaction. Since the stiffness matrix is symmetric, only the lower (or upper) triangle need be actually computed, the rest being loaded from symmetry.

The natural frequencies and eigenvectors are calculated by the Jacobi subroutine [3] using a 16-bit-word mini-computer. Core requirements (including graphics software) fit within a 32 K word partition.

Presentation of Mode Shapes

Upon exit of the eigenroutine, the eigenvectors are stored columnwise in the solution array. These represent normalized relative displacements of the components and are arranged in the same order as is used in assembly of the inertia and stiffness matrices: Motion of sun, planets no. 1 through n, carrier, and ring. For each component, displacements are given in the order rotation, X-translation, and Y-translation.

To aid interpretation of planet motion, local coordinate motion (radial and tangential) may also be computed for the planets. (Note: The Global coordinates have been chosen such that planet no. 1 is at 0° and, therefore, its radial motion is along the X-axis and its tangential motion is along the Y-axis: Local and global coordinates are identical for planet no. 1.)

For better visualization of vibrational modes, the mode shapes are superimposed on a representation of sun, planet and ring gear base circles. The equilibrium position is represented by the line of action of each gear mesh between points of tan-

gency on respective base circles, and by radii through these points of tangency. Rotational displacements of these tangency points (computed as $R\theta$ displacements along the line of action) define angular displacements of the planet. Any translation is added to the computed rotational displacements. The equilbrium position of a single planet at arbitrary angle θ is shown in Table 2(a) and illustrated in Fig. 7. Deflections from equilibrium due to rotation are shown in Table 2(b).

Verification of Method

To validate the algorithm presented above, results were compared with those of earlier studies. Cunliffe[1] performed analytical and experimental studies on a small star gear box with the ring gear rigidly fixed in translation and the carrier fixed in both rotation and translation, thus eliminating 5 degrees of freedom from the 18 degrees of freedom model. Using the Cunliffe data (suppressing the unwanted modes with extremely high - 10^{30} - stiffness values), 5 axisymmetric modes and 4 orthogonal pairs of asymmetric modes were duplicated. As an example, the highest (torsional) mode (which exhibits antisynchronous motion at the sun/planet mesh) is shown in Fig. 8.

Botman[2] investigated an 18 degrees of freedom planetary gear system to obtain 6 symmetric modes and 6 pairs of asymmetric modes. Similar results are obtained in the present work. The 18 modes are described in Table 3. Two of the highest modes obtained with the Botman model are presented in Figs. 9(a) and 10(a). These are very similar to the Cunliffe 13 degrees of freedom torsional modes despite differences in relative sizes of the components and in the additional degrees of freedom.

Results and Discussion

The algorithm developed in this investigation was used to perform a series of comparative parametric studies to assess the effect of unequal mesh stiffnesses on the natural frequencies and the respective mode shapes for a planetary gear system. Three cases are reported: (1) All six mesh stiffnesses equal; (2) One sun/planet stiffness reduced (to one half the nominal value); (3) One planet/ring mesh stiffness reduced. Brief consideration was also given to simultaneous stiffness reductions at two meshes to simulate variation in number of teeth in contact.

Figure 9 shows the highest axisymmetric mode (No. 18 in Table 3) which exhibits anti-synchronous motion of the planets with respect to the sun and ring gears. In Fig. 9(a) all mesh stiffnesses are equal (case 1). Figure 9(b) illustrates the effect of reducing one sun/planet mesh stiffness (case 2). Figure 9(c) shows the effect of reducing one planet/ring mesh stiffness (case 3). Figure 10 illustrates cases 1, 2, and 3 respectively for one of the orthogonal pair of related asymmetric modes (No. 16 in Table 3). Figure 10(b) is particularly affected by the reduced stiffness at the sun mesh which allows significant lateral motion of one planet.

Although some mode shapes changed noticeably due to unequal stiffnesses, the values of the natural frequencies were little affected, varying less than 5 percent for a 50 percent reduction in the stiffness at one mesh. This indicates that the eigenvalues computed from average stiffnesses are a good approximation for the forced response solution of a dynamic system which has time varying stiffnesses due to the alternation between one and two pairs of teeth in mesh.

Natural frequencies were used to determine the time step and total integration time for the numerical calculation of dynamic load factors (Eq. (1) with time-varying, periodic stiffnesses and without the assumption of zero damping). The dynamic load factor is defined as the ratio between the maximum instantaneous load and the static transmitted (design) load. Five percent of the system's shortest natural period provided a stable time step for the integration process. To assure the decay of start-up transients, the integration was carried out for ten times the longest natural period.

Figure 11 shows the variation in the dynamic load factor for one sun/planet and one planet/ring mesh engagement for the planetary gear system outlined in Table 4. The peak dynamic load factor occurs near the frequency of the highest mode found by the eigenvalue method outlined above and is excited by the tooth meshing frequency. Identification of this resonance frequency is particularly important since (for the design analyzed here) dynamic factors above 2.5 are indicative of tooth separation, and constitute an unacceptable operating condition.

Summary of Results

An algorithm suitable for a mini-computer was developed for finding the natural frequencies and mode shapes of a planetary gear system which has unequal stiffnesses between the sun/planet and planet/ring gear meshes. Mode shapes are represented in the form of graphical computer output that illustrates the lateral and rotational motion of the three co-axial gears and the planet gears. This procedure permits the analysis of gear trains utilizing non-uniform mesh conditions and user specified masses, stiffnesses, and boundary conditions. Numerical integration of the equations of motion for a three planetary gear systems was performed. The following results were obtained:

1. Excellent agreement was obtained between natural frequencies calculated assuming constant mesh stiffnesses and resonant frequencies of the dynamic system.

2. The algorithm can be used for determining the time step and total integration times in the numerical solution of the differential equations of motion.

3. The methodology is a quick and efficient means of identifying operating resonance regions and analytically tuning the drive train by examining the effect of parameters such as planet and sun gear support stiffnesses, input/output shaft stiffnesses, and gear mesh stiffnesses.

4. The algorithm is adaptable for use in a Computer-Aided Design (CAD) environment.

References

1. Cunliffe, F.; Smith, J. D.; and Welbourn, D. B.: Dynamic Tooth Loads in Epicyclic Gears. J. Eng. Ind., vol. 96, no. 2, May 1974.

2. Botman, M.: Epicylic Gear Vibration. J. Eng. Ind., vol. 98, no. 3, Aug. 1976, pp. 811-815.

3. Bathe, K.; and Wilson, E. L.: Numerical Methods in Finite Element Analysis. Prentice-Hall, Inc., 1976, pp. 445-460.

TABLE 1. - STIFFNESS TERMS

(a) Bearing support reactions.

Component	Displacement	T/q	F_x/q	F_y/q
Sun	θ_s	$-KT_s$	$-K_s$	$-K_s$
Planet-j	θ_j	0	$-K_p$	$-K_p$
Carrier	θ_c	$-KT_c$	$-K_c$	$-K_c$
Ring	θ_r	$-KT_r$	$-K_r$	$-K_r$

(b) Sun/planet interaction.

Component	Displacement	T/q	F_x/q	F_y/q
Sun	$R_s\theta_s - R_p\theta_j$	$-KSP\ R_s$	$-KSP\ \cos\alpha$	$-KSP\ \sin\alpha$
	$X_s - X_j$	$-KSP\ R_s\ \cos\alpha$	$-KSP\ \cos^2\alpha$	$-KSP\ \cos\alpha\ \sin\alpha$
	$Y_s - Y_j$	$-KSP\ \sin\alpha$	$-KSP\ \cos\alpha\ \sin\alpha$	$-KSP\ \sin^2\alpha$
Planet "j"	$R_p\theta_j - R_s\theta_s$	$-KSP\ R_p$	$-KSP\ \cos\alpha$	$-KSP\ \sin\alpha$
	$X_j - X_s$	$-KSP\ R_p\ \cos\alpha$	$-KSP\ \cos^2\alpha$	$-KSP\ \cos\alpha\ \sin\alpha$
	$Y_j - Y_s$	$-KSP\ R_p\ \sin\alpha$	$-KSP\ \cos\alpha\ \sin\alpha$	$-KSP\ \sin^2\alpha$

(c) Carrier/planet interaction.

Component	Displacement	T/q	F_x/q	F_y/q
Carrier	θ_c	$-K_pR_c^2$	$+K_pR_c\ \sin\beta$	$-K_pR_c\ \cos\beta$
	$X_c - X_j$	$+K_pR_c\ \sin\beta$	$-K_pR_c$	0
	$Y_c - Y_j$	$-K_pR_c\ \cos\beta$	0	$-K_pR_c$
Planet "j"	θ_c	0	$-K_pR_c\ \sin\beta$	$+K_pR_c\ \cos\beta$
	$X_j - X_c$	0	$-K_p$	0
	$Y_j - Y_c$	0	0	$-K_p$

(d) Ring/planet interaction.

Component	Displacement	T/q	F_x/q	F_y/q
Ring	$R_r\theta_r - R_p\theta_j$	$-KPR\ R_r$	$+KPR\ \cos\gamma$	$+KPR\ \sin\gamma$
	$X_r - X_j$	$+KPR\ R_r\ \cos\gamma$	$-KPR\ \cos^2\gamma$	$-KPR\ \cos\gamma\ \sin\gamma$
	$Y_r - Y_j$	$+KPR\ R_r\ \sin\gamma$	$-KPR\ \cos\gamma\ \sin\gamma$	$-KPR\ \sin^2\gamma$
Planet "j"	$R_p\theta_j - R_r\theta_r$	$-KPR\ R_p$	$+KPR\ \cos\gamma$	$+KPR\ \sin\gamma$
	$X_j - X_r$	$+KPR\ R_p\ \cos\gamma$	$-KPR\ \cos^2\gamma$	$-KPR\ \cos\gamma\ \sin\gamma$
	$Y_j - Y_r$	$+KPR\ R_p\ \sin\gamma$	$-KPR\ \cos\gamma\ \sin\gamma$	$-KPR\ \sin^2\gamma$

TABLE 2. - MODE SHAPES

(a) Equilibrium position: center and base circle tangency points.

No.	Location	X-coordinate	Y-coordinate
1	Sun/"j" tang.	$R_s \sin \alpha$	$-R_s \cos \alpha$
2	"j"/sun tang.	$R_c \cos \beta - R_p \sin \alpha$	$R_c \sin \beta + R_p \cos \alpha$
3	"j" center	$R_c \cos \beta$	$R_c \sin \beta$
4	"j"/ring tang.	$R_c \cos \beta + R_p \sin \gamma$	$R_c \sin \beta - R_p \cos \gamma$
5	Ring/"j" tang.	$R_r \sin \gamma$	$-R_r \cos \gamma$

(b) Deflection at tangency points due to component rotation.

No.	Location	X-deflection	Y-deflection
1	Sun/"j" tang.	$R_s \cos \alpha\theta_s$	$R_s \sin \alpha\theta_s$
2	"j"/sun tang.	$R_p \cos \alpha\theta_p$	$R_p \sin \alpha\theta_p$
3	"j" center	0	0
4	"j"/ring tang.	$-R_p \cos \gamma\theta_p$	$-R_p \sin \gamma\theta_p$
5	Ring/"j" tang.	$-R_r \cos \gamma\theta_r$	$-R_r \sin \gamma\theta_r$

TABLE 3. - DESCRIPTION OF MODE SHAPES

Mode no.	Type	Motion	Strain energy
1a, 1b	Translational	Sun	Sun mesh
3	Symmetric		
4	Symmetric	Ring, carrier	Ring mesh, output shaft
5a, 5b	Translational		
7a, 7b	Translational	Radial planet motion	Planet bearings
9	Symmetric		
10	Symmetric	Carrier, sun	Output shaft
11a, 11b	Translational		
13a, 13b	Translational	Tangential planet motion	Ring mesh, planet bearings
15	Symmetric		
16a, 16b	Translational	Antisynchronous motion	Sun mesh, ring mesh
18	Symmetric		

TABLE 4. - DESIGN AND SYSTEM PARAMETERS USED FOR CALCULATING DYNAMIC FACTORS

Design Parameters	
Diametral pitch	5
Pressure angle, deg	22.5
Number of teeth	
Sun	25
Planet	24
Ring	73
Face width, in.	1
Theoretical contact ratio	
Sun/planet	1.56
Planet/ring	1.78
System Properties	
J_{driver}, in-lb•sec^2	5.000
J_{sun}, in-lb•sec^2	0.040
M_{sun}, lb•sec^2/in	0.015
J_{planet}, in-lb•sec^2	0.033
J_{ring}, in-lb•sec^2	2.000
J_{load}, in-lb•sec^2	5.000

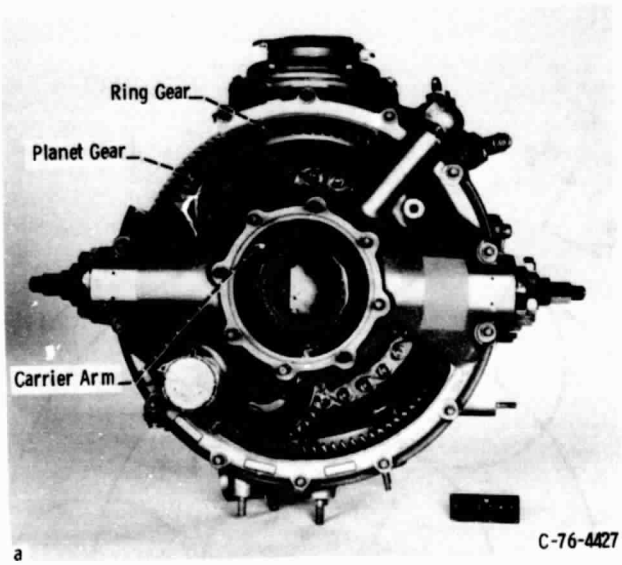

a

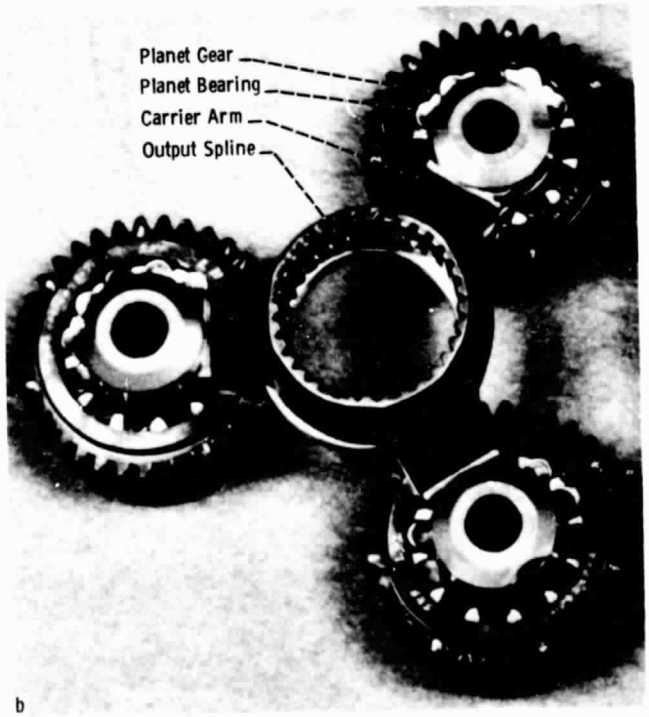

b

(a) Partial cutaway.
(b) Detail, planet carrier assembly.
Figure 1. - Planetary gear train.

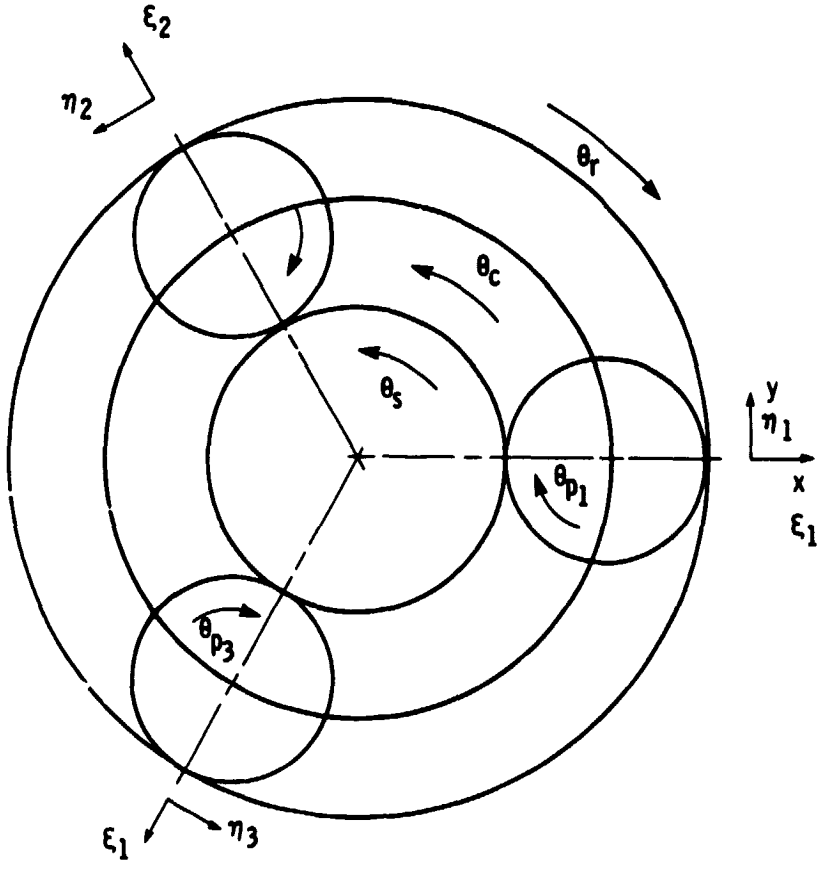

Figure 2. - Planetary gear stage showing global and local coordinate systems The direction of positive rotation for each component is indicated by arrows.

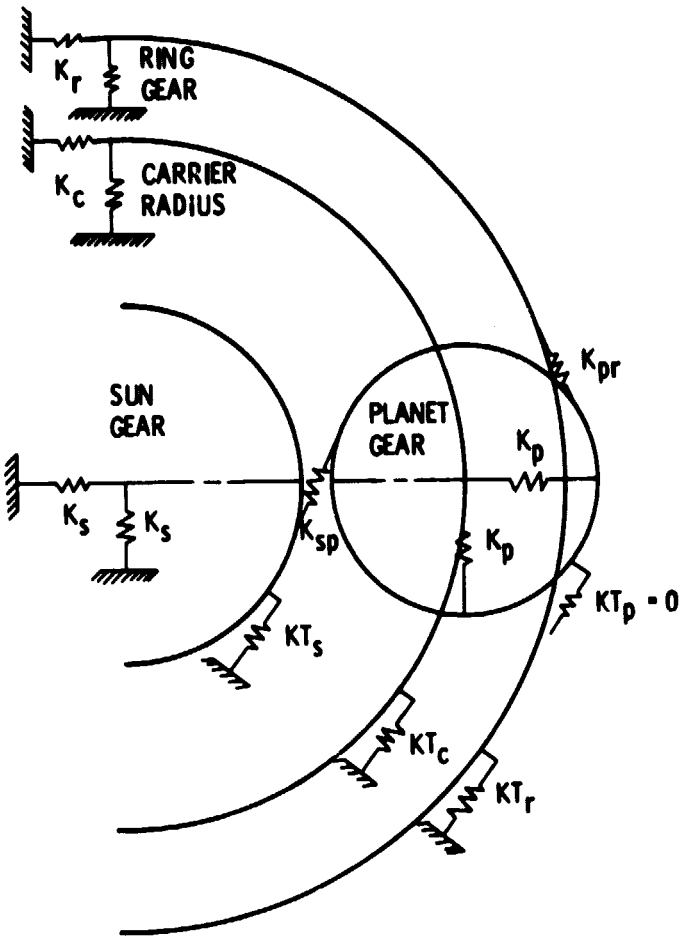

Figure 3. - Dynamic model of planetary gear system.

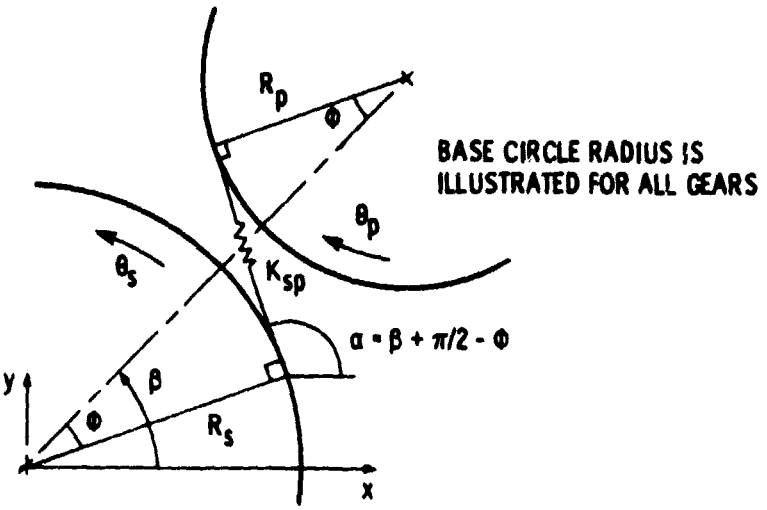

Figure 4. - Sun-planet interaction for planet "j" at arbitrary angle β.

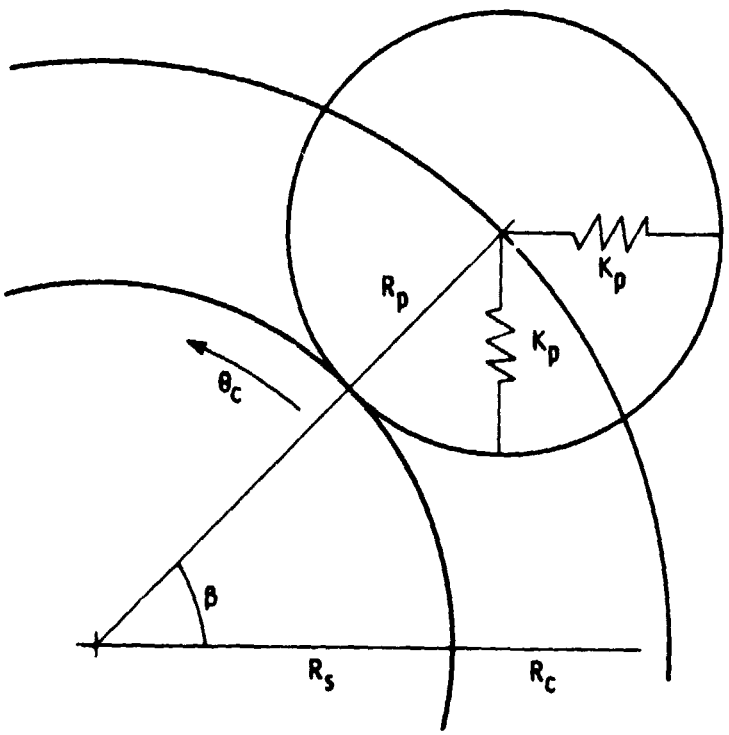

Figure 5. - Carrier-planet interaction for planet "j" at arbitrary angle β.

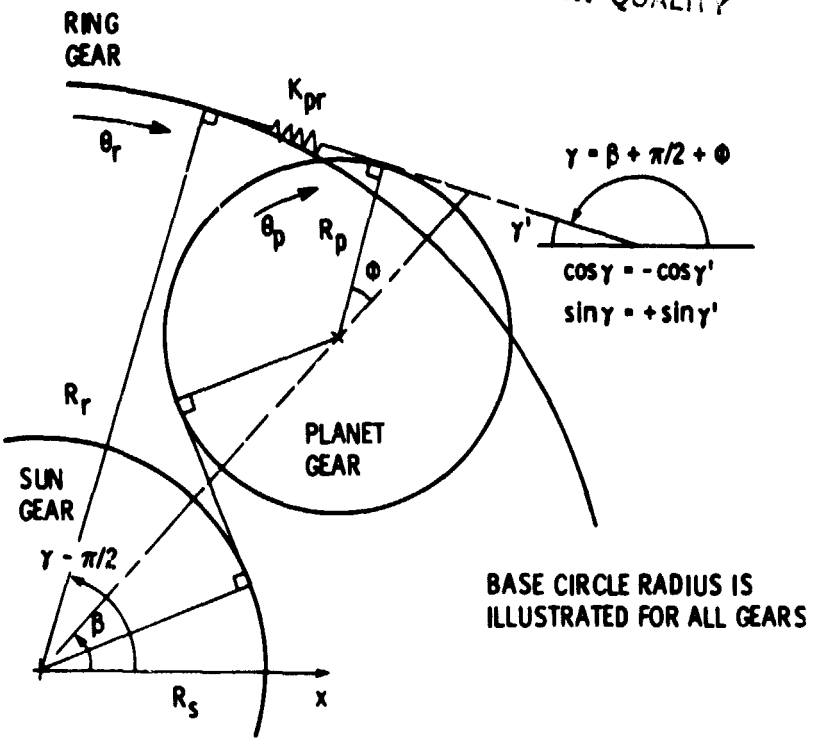

Figure 6. - Ring-planet interaction for planet "j" at arbitrary angle β.

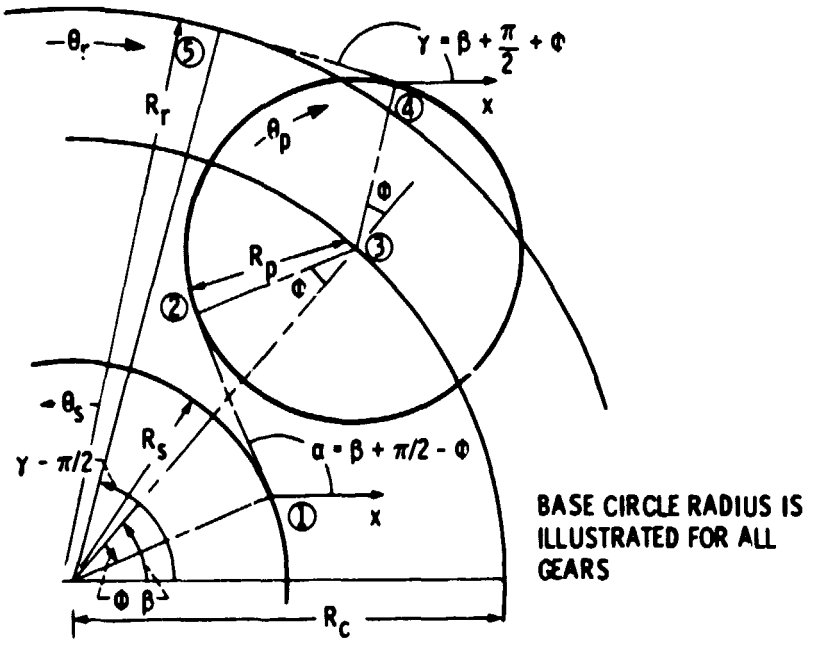

Figure 7. - Equilibrium position of planet "J" at arbitrary angle β. The direction of positive rotation for sun, planet and ring gears is indicated by arrows.

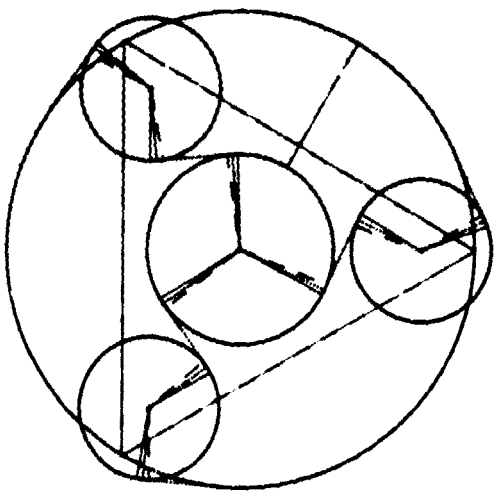

Figure 8. - 13 DOF Antisynchronous symmetric mode.

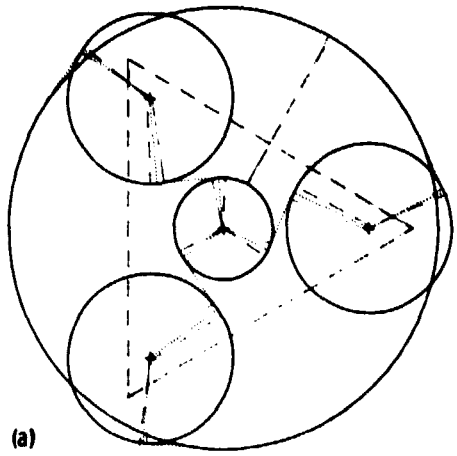

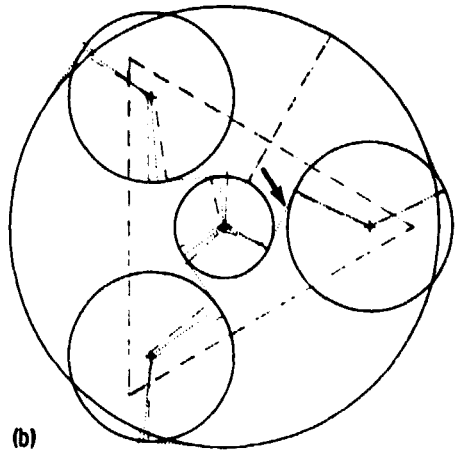

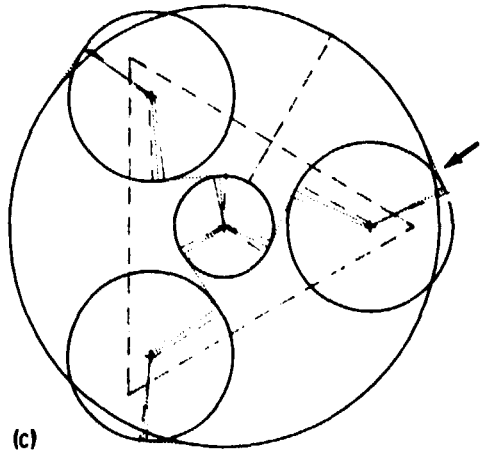

(a) All mesh stiffnesses equal.
(b) One sun/planet mesh stiffness reduced.
(c) One planet/ring mesh stiffness reduced.

Figure 9. - 18 DOF Antisynchronous symmetric mode.

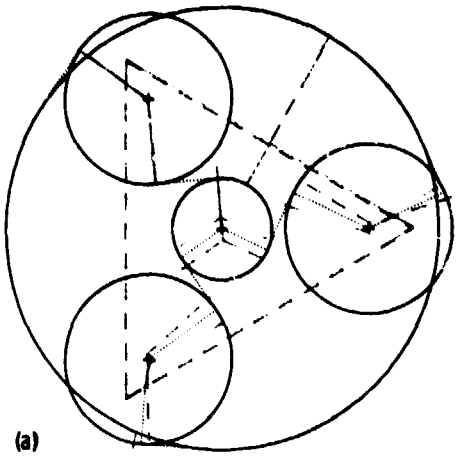

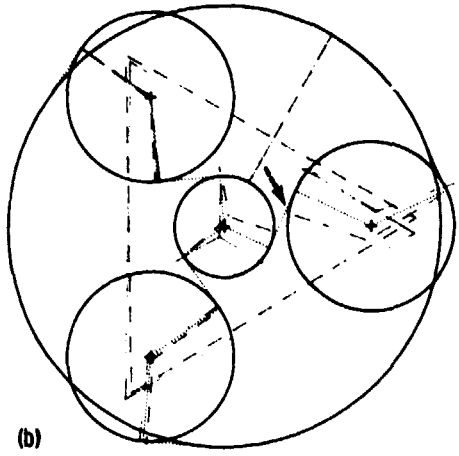

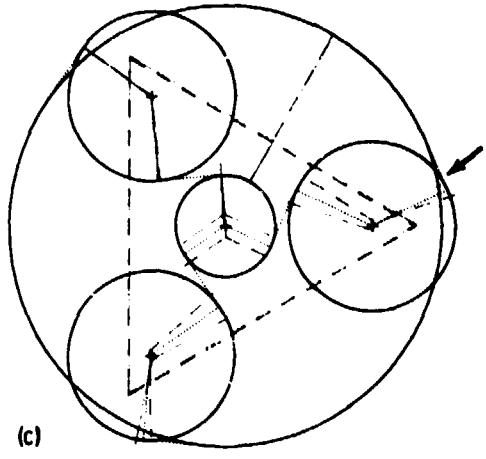

(a) All mesh stiffnesses equal.
(b) One sun/planet mesh stiffness reduced.
(c) One planet/ring mesh stiffness reduced.

Figure 10. - 18 DOF Antisynchronous translational mode.

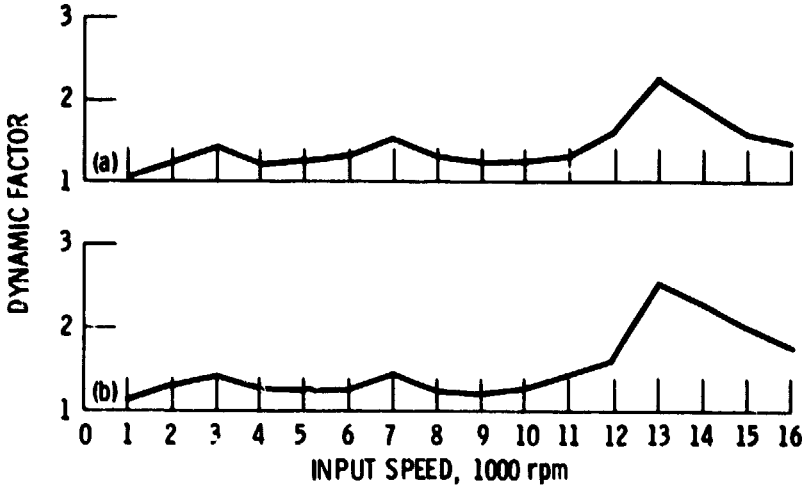

(a) Sun/planet mesh.
(b) Planet/ring mesh.

Figure 11. - Dynamic factor as a function of sun input speed.